ORIGINAL PAPER

Electrochemical degradation of the Acid Blue 62 dye on a β-PbO$_2$ anode assessed by the response surface methodology

**José M. Aquino · Romeu C. Rocha-Filho ·
Nerilso Bocchi · Sonia R. Biaggio**

Abstract The electrochemical degradation of the anthraquinonic dye Acid Blue 62 in a filter-press reactor on a Ti/Pt/ β-PbO$_2$ anode was investigated using the response surface methodology with the variables: current density, pH, [NaCl], and temperature. The system's modeling was carried out with the charge required for 90% decolorization (Q^{90}) and the chemical oxygen demand removal percentage after a 30 min electrolysis (COD^{30}), with good correlations between predicted and observed values. Best conditions for decolorization were attained in acidic solutions (pH = 4) with medium to high [NaCl] (1.0–2.0 g L^{-1}) and lower temperature due to the prevalent oxidant species HOCl and Cl$_2$. Optimal conditions for COD^{30} removal were attained at high current densities in pH > 5 solutions with high [NaCl], when the prevalent oxidant species are HOCl and OCl$^-$. The lowest charge per unit volume of the electrolyzed solution necessary for total mineralization was attained at pH 11.

Keywords Electrooxidation ·
Dye degradation in the presence of chlorine ·
Acid Blue 62 dye · PbO$_2$ anode · Factorial design

1 Introduction

Synthetic dyes are a class of organic compounds extensively used for innumerable industrial applications, mainly textile. Among these compounds, the azo (–N=N–) ones are the most produced and consumed in dyeing processes, but other classes of dyes such as the anthraquinonic ones are also used [1]. As a consequence of their use, significant quantities of effluents are produced and have to be treated before disposal into the environment. Textile effluents are mainly characterized by intense colors originated by non-reacted dyestuff and high organic loads (due to the presence of auxiliary chemicals). The presence of synthetic dyes in water can interfere with sun light penetration [2] and cause health risks [1, 3, 4]. Furthermore, dye molecules are known to be stable and thus may remain in the environment for long periods [3]. Hence, the use and implementation of various methods to decolorize and degrade synthetic dyes are of great importance, due to increasingly rigid environmental regulations [5].

As described in the literature [1, 6, 7], there are several methods for the remediation of textile effluents, such as: biological, chemical, physico-chemical, advanced oxidation, and electrochemical processes. Among them, electrochemical methods [1, 8, 9] might be a reasonable option due to the combination of easy implementation with pollutants high removal rates. Their main drawback regards the use of electrical energy. However, the development of new electrode materials with a high oxidation power can lead to better efficiencies for the removal of pollutants. In conventional electrooxidation, pollutants can be removed by: (i) direct oxidation, through the direct transfer of electrons from the adsorbed pollutant on the electrode surface and (ii) indirect oxidation, in which electrons are transferred to other species adsorbed on the electrode surface [9]. The most common electrogenerated species in indirect oxidation (anodic process) is the hydroxyl radical (•OH). According to the interaction between this radical and anode materials, Kapalka et al. [10] classified them from low to high oxidation power anodes. Furthermore, when chloride ions are used, the pollutants oxidation may

J. M. Aquino · R. C. Rocha-Filho (✉) · N. Bocchi ·
S. R. Biaggio
Departamento de Química, Universidade Federal de São Carlos,
C.P. 676, 13560-970 São Carlos, SP, Brazil
e-mail: romeu@ufscar.br

also be mediated by other species like Cl_2, ClO^-, and HClO [9, 11, 12].

Lead dioxide (PbO_2) anodes are an alternative to the boron-doped diamond (BDD) or conventional dimensionally stable (DSA) anodes due to the combination of easiness of preparation [9], medium to high oxidation power [10], and low cost [13–15]. The electrochemical performance and stability of PbO_2 anodes are strongly related to substrate preparation [16–18] and may be influenced by doping species, as studied by Andrade et al. [13].

Modeling the performance of an experimental system, considering its variables, is useful because it enables to find and optimize the best experimental conditions [19]. Moreover, it is possible to extract explicit relationships and tendencies between variables. Thus, statistical methodologies like the response surface methodology (RSM) are powerful techniques that permit studying and modeling a specific system, as it has been carried out, for instance, for the electrooxidation of the Reactive Red 141 dye [20].

The degradation or removal of the Acid Blue 62 (AB 62) anthraquinonic dye from solution has almost not been investigated, and the existing few papers concern either adsorption, biological, or advanced oxidation processes [21–23]. Therefore, the purpose of this work is to find the best experimental conditions, using RSM, for the electrochemical degradation of the AB 62 dye on a Ti–Pt/β-PbO_2 anode.

2 Experimental

2.1 Chemicals

All chemicals, including $Pb(NO_3)_2$ (a.r., Acros), sodium lauryl sulfate, SLS (99%, Fisher Scientific), H_2PtCl_6 (99.9%, Aldrich), HCl (36.5%, Mallinckrodt), H_2SO_4 (98%, Mallinckrodt), HNO_3 (69–70%, Mallinckrodt), Ag_2SO_4 (a.r., JT Baker), $HgSO_4$ (a.r., JT Baker), NaCl (a.r., JT Baker), Na_2SO_4 (a.r., Qhemis), and AB 62 (Quimanil), were used as received. Doubly deionized water (Millipore Milli-Q system, $\geq$18.2 MΩ cm) was used for the preparation of all solutions.

2.2 β-PbO_2 film preparation on a Ti–Pt substrate

The β-PbO_2 films were electrodeposited on a platinized Ti substrate in a conventional electrochemical cell, using a calomel reference electrode and two AISI-304 stainless steel plates as counter electrodes. The procedures involving the Ti substrate platinization and the β-PbO_2 film preparation are fully described in a previous work [20].

2.3 Electrochemical degradation of the AB 62 dye

The electrochemical experiments were carried out in a one-compartment filter-press reactor composed of the Ti–Pt/β-PbO_2 anode (exposed area: 3.1×1.9 cm, each face) and two nickel plates as cathodes. Details about the experimental setup and the electrochemical reactor are also reported in a previous work [20]. A central composite design (CCD) coupled with RSM [19] was used in the AB 62 dye electrochemical degradation. The variables current density (j), pH, NaCl concentration ([NaCl]), and temperature (θ) were investigated at five different levels (-2, -1, 0, 1, 2); Table 1 shows the used ranges and levels for these variables. Three replications were carried out at the design center in order to evaluate the pure error and, consequently, the lack of fit. All the experiments were carried out randomly using 0.4 L of a 0.1 mol L^{-1} Na_2SO_4 aqueous solution containing a fixed concentration (100 mg L^{-1}) of the AB 62 dye, at a flow rate of 360 L h^{-1} (0.5 m s^{-1}).

2.4 Analyses

The time evolutions of the solution chemical oxygen demand (COD) and color were used to analyze the system's electrochemical performance. The dye decolorization was monitored in situ (at 640 nm) by circulating the dye-containing solution between the electrochemical system reservoir and an UV–vis spectrophotometer (ULTROSPEC 2100pro, from Amersham Pharmacia Biotech). The performance of the electrochemical system was modeled based on the charge per unit volume of the electrolyzed solution required for 90% decolorization (Q^{90}) and on the COD removal values after 30 min of electrolysis (COD^{30}). The COD^{30} measurements (described in detail elsewhere

Table 1 Range and codification of the independent variables (X_i) used in the experimental design

Independent variables	Coded levels and corresponding values				
	-2	-1	0	1	2
Current density (j), X_1 (mA cm^{-2})	25	50	75	100	125
pH, X_2	2.5	4	5.5	7	8.5
NaCl concentration, X_3 (g L^{-1})	0	0.58	1.17	1.75	2.34
Temperature (θ), X_4 (°C)	15	25	35	45	55

[20]) were carried out using 2.5 mL samples of the electrolyzed dye solution.

The linear and quadratic equations used to model the RSM responses were $Y = \beta_0 + \Sigma\beta_i X_i$ and $Y = \beta_0 + \Sigma\beta_i X_i + \Sigma\beta_{ii}X_i^2 + \Sigma\beta_{ij}X_i X_j$, respectively, where $\beta_{0,i,ii,ij}$ are model coefficients and $X_{i,j}$ the independent variables. Detailed description and discussion of these equations can be found, for instance, in Montgomery's book [19].

3 Results and discussion

The CCD matrix along with the predicted and observed Q^{90} and COD^{30} values for the electrooxidation of the AB 62 dye are shown in Table 2. Firstly, the behavior of both these variables was modeled using a quadratic equation. However, for Q^{90} the obtained results were inadequate because they presented a considerable lack of fit due to the

high values of the residues, thus failing to predict the charge quantitatively; this led to the use of a linear equation with good results, but prevented any prediction for the axial part of the CCD matrix.

The modeling equations that best describe the Q^{90} and the COD^{30} behaviors are given below. Non-significant coefficients were excluded from these equations taking into account the analysis of variance (ANOVA) and the Student's t test (at 95% confidence level).

$$Q^{90} = 0.402 + 0.094X_2 - 0.146X_3 + 0.078X_4 \qquad (1)$$

$$\begin{aligned} COD^{30} = {}& 55.22 + 8.76X_1 + 3.27X_2 + 6.44X_3 + 4.76X_4 \\ & - 3.00X_1^2 - 4.48X_2^2 - 4.19X_3^2 + 1.73X_1X_2 \\ & - 3.04X_1X_4 + 2.10X_2X_3 + 2.48X_3X_4 \end{aligned} \qquad (2)$$

The Q^{90} behavior modeled using Eq. 1 presented no lack of fit, according to the F-test. As it can be seen in Fig. 1a, the predicted and observed Q^{90} values are well

Table 2 Central composite design matrix for investigation of best conditions in the electrooxidation of the Acid Blue 62 dye and respective predicted and observed charges (for 90% decolorization) and COD removal values (after a 30 min electrolysis), as well as energy consumption per unit volume of the electrolyzed solution associated to observed Q^{90} (EC)

Exp	j	pH	[NaCl]	θ	Q^{90}(A h L^{-1})		COD^{30} removal (%)		EC (kW h m^{-3})
					Predicted	Observed	Predicted	Observed	
1	−1	−1	−1	−1	0.375	0.343	23.6	15.8	1.85
2	1	−1	−1	−1	0.375	0.226	43.7	39.8	1.60
3	−1	1	−1	−1	0.564	0.551	22.5	27.9	3.05
4	1	1	−1	−1	0.564	0.696	49.5	41.1	5.20
5	−1	−1	1	−1	0.084	0.123	27.3	24.5	0.64
6	1	−1	1	−1	0.084	0.147	47.5	51.3	1.03
7	−1	1	1	−1	0.273	0.252	34.6	39.3	1.31
8	1	1	1	−1	0.273	0.319	61.7	46.5	2.22
9	−1	−1	−1	1	0.531	0.613	34.2	45.6	3.15
10	1	−1	−1	1	0.531	0.500	42.2	41.6	3.04
11	−1	1	−1	1	0.720	0.681	33.1	33.3	3.36
12	1	1	−1	1	0.720	0.834	48.0	50.4	5.18
13	−1	−1	1	1	0.239	0.203	47.9	60.3	0.93
14	1	−1	1	1	0.239	0.368	55.9	46.6	2.16
15	−1	1	1	1	0.428	0.421	55.1	58.6	1.90
16	1	1	1	1	0.428	0.280	70.1	81.9	1.60
17	0	0	0	0	0.402	0.357	55.2	49.6	2.09
18	0	0	0	0	0.402	0.383	55.2	63.8	2.22
19	0	0	0	0	0.402	0.338	55.2	52.3	1.93
20	−2	0	0	0	–	0.425	25.7	12.6	1.69
21	2	0	0	0	–	0.294	60.7	70.9	2.10
22	0	−2	0	0	–	0.184	30.8	29.6	1.05
23	0	2	0	0	–	0.364	43.9	42.1	2.12
24	0	0	−2	0	–	2.954	25.6	26.7	18.32
25	0	0	2	0	–	0.199	51.3	47.2	1.12
26	0	0	0	−2	–	0.276	45.7	57.1	1.87
27	0	0	0	2	–	0.486	64.7	48.2	2.53

correlated; an exact correspondence ($y = 1.000\,x$) could be fitted with $r = 0.912$. The Q^{90} experiments of the axial part of the CCD matrix were carried out and the obtained results are also shown in Table 2 (experiments 20–27; no predicted values, as noted above). As already mentioned, the modeling of COD^{30} by the quadratic Eq. 2 presented no lack of fit, with a good correlation between the predicted and observed values, as shown in Fig. 1b; in this case, a quite good correspondence ($y = 0.975\,x$) could be fitted with $r = 0.852$.

Figure 2 shows some of the response surfaces for Q^{90} as a function of the independent variables pH, [NaCl], and θ (j was excluded due to a non-significant coefficient—see above, Eq. 1). Among these variables, pH is quite important due to the different chloro species prevalent at given pH ranges, as shown by Cheng and Kelsall [11]. Figure 2a (data obtained at 35 °C and using 75 mA cm^{-2}) shows the Q^{90} behavior as a function of [NaCl] and pH; from this response surface one can apprehend that the best conditions for color removal (lower Q^{90} values) are attained at the highest NaCl concentrations and lowest pHs. Similar response surface characteristics were previously obtained

in the electrooxidation of the Reactive Red 141 dye [20]. Electrolyses of increasingly acidic solutions containing NaCl lead to the presence of the Cl_2 and HOCl gaseous species (Cl_2 is predominant at pH < 3, while HOCl is predominant for 3 < pH < 7.5); these species have higher oxidation potentials than the one of the OCl$^-$ species, which becomes the predominant chlorine species only at pH > 7.5 [11, 24]. Hence, one can conclude that an increasing presence of Cl_2 along with HOCl favors the decolorization of the dye.

Figure 2b (data obtained using 1.17 g L^{-1} NaCl, 75 mA cm^{-2}) shows the Q^{90} behavior as a function of temperature and pH; now, one can see that the best conditions for color removal (lower Q^{90} values) are attained at the lowest temperatures and pHs. As discussed above, lower Q^{90} values are favored by the chloro species generated at lower pHs, Cl_2 and HOCl; the concentration of the former increases as the pH becomes lower than five. Furthermore, low pHs combined with low temperatures lead to better conditions for color removal due to the consequent increase in the solubility of these chloro species, that is, the following solubility equilibria involving Cl_2 and HOCl are

Fig. 1 Predicted and observed plot for **a** charge required for 90% decolorization (Q^{90}) and **b** COD removal percentage after a 30 min electrolysis (COD^{30})
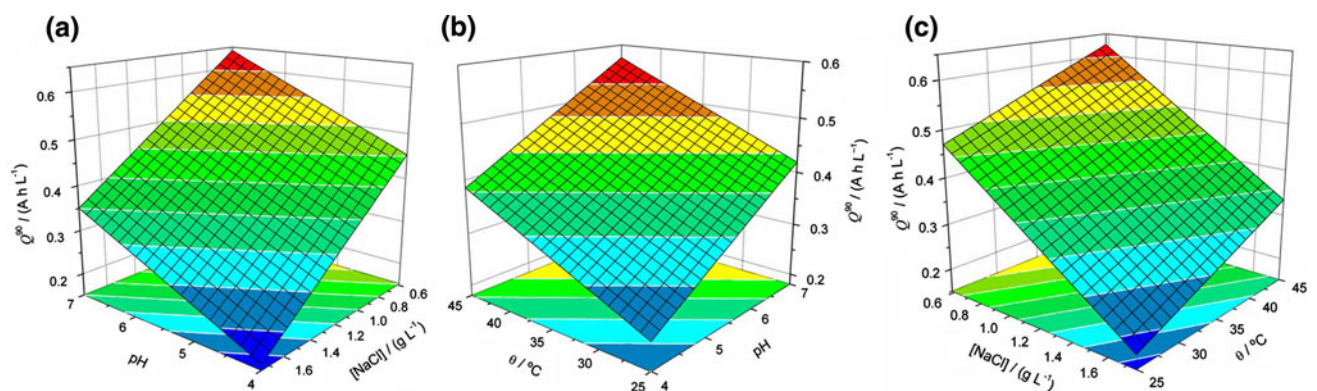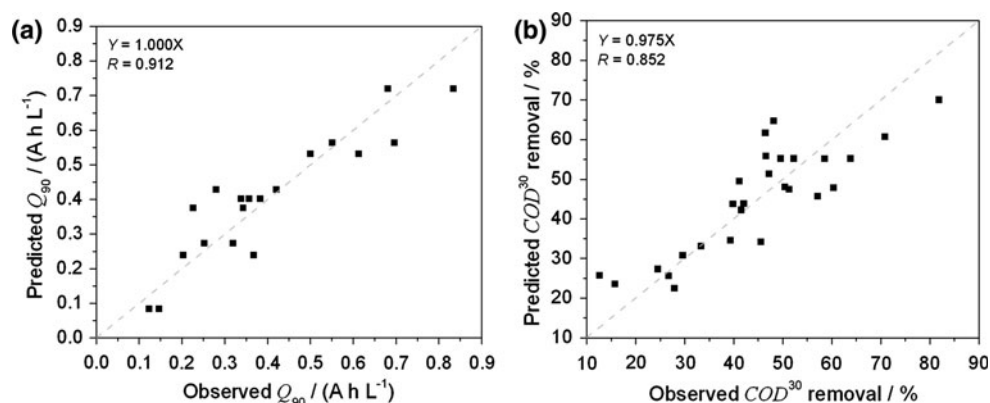
Fig. 2 Response surfaces for the charge required for 90% decolorization (Q^{90}) as a function of **a** pH and NaCl concentration (at 35 °C, using 75 mA cm^{-2}), **b** temperature and pH (using 75 mA cm^{-2}, 1.17 g L^{-1} NaCl), and **c** NaCl concentration and temperature (using 75 mA cm^{-2}, pH 5.5)

dislocated towards the aqueous phase as the temperature is decreased [11, 25]:

$$Cl_2(aq) \leftrightarrows Cl_2(g) \qquad (3)$$

$$HClO(aq) \leftrightarrows HClO(g) \qquad (4)$$

Figure 2c (data obtained at 75 mA cm^{-2}, pH 5.5) confirms that minimum Q^{90} values are attained at the highest NaCl concentrations and the lowest temperatures. This temperature range is consistent with what was discussed above related to the solubility of the chloro species prevalent at pH 5.5, specifically HClO.

The Q^{90} data hereinbefore presented allow concluding that best decolorization conditions are attained at the most acidic conditions and lowest temperatures, which favor the presence of the HOCl and Cl$_2$ species in the solution. On the other hand, by comparing the variation tendencies in Fig. 2a, b, and c, it becomes clear that [NaCl] plays a very important role, since the NaCl concentration in solution directly determines the concentration of the oxidizing chloro species in the solution.

The energy consumption per unit volume of the electrolyzed solution associated to Q^{90} (EC) is also presented in Table 2. The lowest value of EC (0.64 kW h m^{-3}) was attained for experiment five, carried out at 25 °C, applying 50 mA cm^{-2} to a dye solution of pH 4 containing 1.75 g L^{-1} NaCl. This lowest EC value is slightly lower than the one previously obtained for the Reactive Red 141 dye [20].

The response surfaces for COD^{30} are shown in Fig. 3, as a function of the independent variables pH, [NaCl], θ, and j. As already highlighted above, the pH is an important variable in the electrooxidation of dye solutions containing chloride ions; thus, in this figure the pH is used to describe the COD removal along with each of the remaining variables. Figure 3a (data obtained at 35 °C and using 75 mA cm^{-2}) shows the COD^{30} behavior as a function of pH and [NaCl]. Clearly, the best conditions for COD removal are

attained using solutions of pH between 5 and 8 and the highest NaCl concentrations; for most of this pH range HClO is the predominant species, except for pH > 7.5, when OCl$^-$ becomes predominant. The OCl$^-$ species has a lower oxidation potential than those of the Cl$_2$ and HOCl gaseous species, but because the OCl$^-$ concentration might be higher than that of the other chloro species, one expects that greater COD^{30} values be attained when OCl$^-$ is present. Different pH conditions for COD removal and decolorization were also found in a previous work on the electrooxidation of the Reactive Red 141 dye [20].

Figure 3b (data obtained using 75 mA cm^{-2}, 1.17 g L^{-1} NaCl) shows the COD^{30} behavior as a function of pH and temperature. According to this response surface, the best conditions for COD removal are attained using solutions of pH between 5 and 7 and the highest temperatures, although the temperature dependence is not as strong as the one on pH. Actually, the results presented in Table 2 (experiments 26, 27) show that an inverted dependence on temperature was obtained (again not a very strong dependence).

Figure 3c (data obtained at 35 °C, using 1.17 g L^{-1} NaCl) shows the COD^{30} behavior as a function of pH and current density. Clearly, as one may have expected, higher current densities favor the COD removal, especially for pH values greater than five. This behavior is related to the higher amount of chloro species generated at high current densities. Once again, it can be inferred that the presence of the HClO and ClO$^-$ species favor COD removal. A similar response surface was previously obtained in the electrooxidation of the Reactive Red 141 dye, but with a less marked pH dependence [20].

In order to find the best condition (maximum value) for COD removal at 30 min of electrolysis, the COD^{30} equation was independently derived in relation to each of the four independent variables $X_{i,j}$ (for $1 \leq i, j \leq 4$) and then equaled to zero, that is:
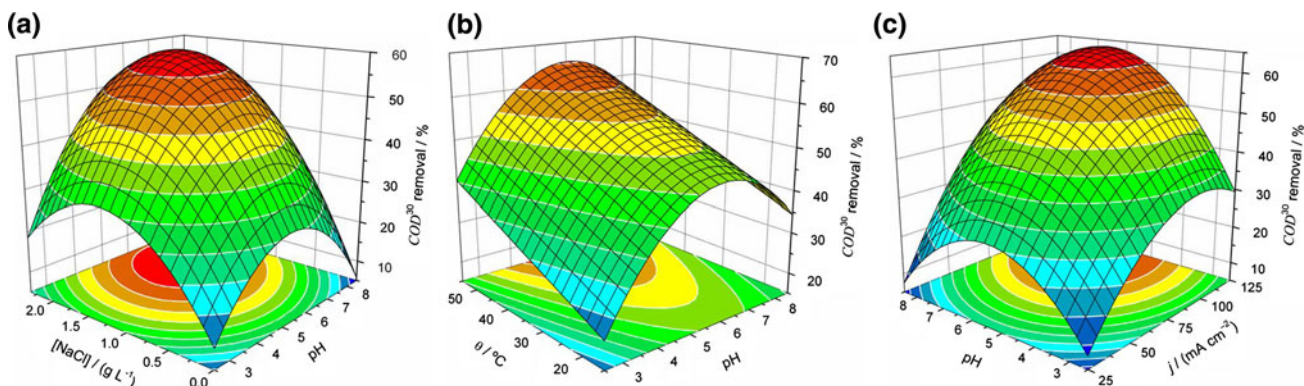
Fig. 3 Response surfaces for the COD removal percentage after a 30 min electrolysis (COD^{30}) as a function of **a** NaCl concentration and pH (at 35 °C, using 75 mA cm^{-2}), **b** temperature and pH (using 75 mA cm^{-2}, 1.17 g L^{-1} NaCl), and **c** pH and current density (at 35 °C, using 1.17 g L^{-1} NaCl)

$$\left(\frac{\partial COD^{30}}{\partial X_i}\right)_{X_{j\neq i}} = 0$$

The best condition resulting from this derivation is shown in Table 3 as COD_{max}. Considering that this condition was obtained without taking into account the energy consumption, an additional condition was determined in order to compare the COD_{max} condition with the one that yielded the lowest value for the ratio between the energy consumption for Q^{90} (EC) and the COD^{30} (values listed in Table 2) —identified as condition $(EC/COD^{30})_{min,pH4}$ in Table 3. Then, additional experiments were carried out for these two conditions, until total mineralization of the dye. As it can be seen in Fig. 4a, the condition COD_{max} resulted in a COD^{30} value of 86%, whereas that for $(EC/COD^{30})_{min,pH4}$ yielded a COD^{30} value of about 60%; hence, the condition COD_{max} resulted in faster total mineralization. However, when the charges per unit volume of the electrolyzed dye solution (Q) required to attain these two COD^{30} values are compared, the best performance is the one obtained using the condition $(EC/COD^{30})_{min,pH4}$, as shown in Fig. 4b; hence, the condition $(EC/COD^{30})_{min,pH4}$ resulted in a smaller energy consumption to reach total mineralization of the AB 62 dye, when the predominant species in solution is HClO, accompanied by Cl_2.

Considering that the presence of the ClO^- species might favor the mineralization of the dye, as indicated by the data shown in Fig. 3, another important comparison also related to the $(EC/COD^{30})_{min,pH4}$ condition was carried out focusing specifically on the effect of pH on the total mineralization of the dye; thus, additional experiments were carried out at pH 11 —identified as condition $(EC/COD^{30})_{min,pH11}$ in Table 3, when ClO^- is the sole chloro species in solution. As it can be seen in Fig. 4b, at pH 11 the total mineralization of the AB 62 dye is attained at even smaller Q values (1.47 A h L^{-1}) than at pH 4 (2.21 A h L^{-1}), despite the initial high removal rate at the latter pH value. These different behaviors are related to the different chloro species present in the acidic (mostly HClO along with Cl_2) and basic (solely OCl^-) solutions, as well as to the differences in the stability of these species in solution with the temperature.

4 Conclusions

The use of RSM enabled studying and modeling the influence of a high number of variables, with a limited number of experiments, in order to find the best conditions for removal of color (charge per unit volume of the electrolyzed solution required for 90% decolorization) and COD (value after 30 min of electrolysis—COD^{30}) during the electrooxidation of the AB 62 dye in the presence of chloride ions. The obtained results indicate that different conditions are needed for color and COD removals, which depend mainly on the solution pH and temperature during the electrolysis: (i) acidic solutions at lower temperatures favor the dye decolorization due to the prevalence of the Cl_2 and HClO gaseous species, which are strong oxidants for the dye chromophore; (ii) less acidic to basic solutions at higher temperatures lead to a higher COD removal because of the increasing presence of the OCl^- species, which, despite being a less strong oxidant, may be present in higher concentrations than the ones possible for the other gaseous chloro species present in the more acidic solutions. Finally, a mathematical derivation of the COD^{30} model yielded the best conditions to attain maximum COD^{30} values (or total mineralization of the dye). However, these conditions are not economically feasible in comparison to

Table 3 Values of current density, pH, NaCl concentration, and temperature for COD monitoring at specific conditions (see text)

Condition	j (mA cm^{-2})	pH	[NaCl] (g L^{-1})	θ (°C)
COD_{max}	125	6.9	1.62	27
$(EC/COD^{30})_{min,pH4}$	50	4	1.75	45
$(EC/COD^{30})_{min,pH11}$	50	11	1.75	45

Fig. 4 COD monitoring as a function of **a** time and **b** applied charge. The curves are associated with the best conditions obtained by derivation of the mathematical model for COD^{30} (COD_{max}) and to the best conditions (lowest values) for the ratio EC/COD^{30} at pH 4 and 11 (see text)
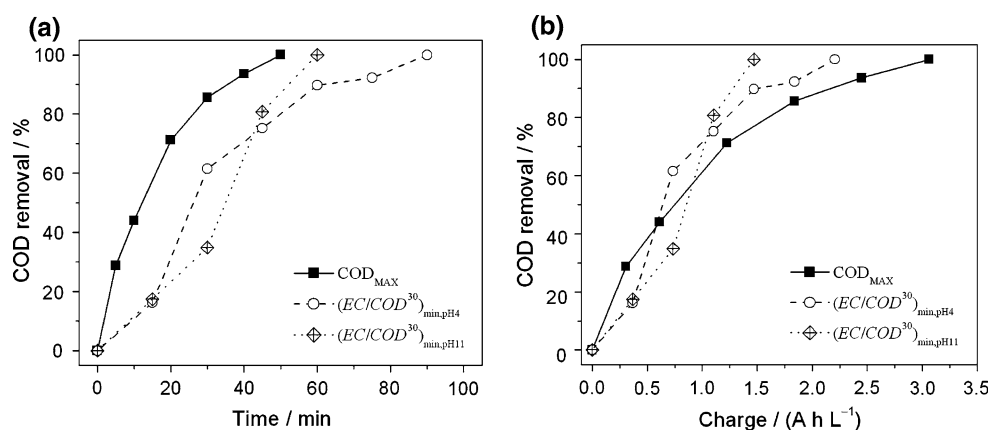
the ones that yielded the lowest value for the ratio between the energy consumption at 90% color removal and the COD^{30}, which involve using a lower current density value at pH 4, thus leading to a lower charge per unit volume of the electrolyzed dye solution to attain total mineralization; moreover, this charge becomes much lower yet when the solution pH is changed to 11 (when ClO^- is the sole chloro species present in solution), a result that is coherent with the findings about the best conditions for COD removal.

References

1. Martínez-Huitle CA, Brillas E (2009) Appl Catal B 87:105
2. Muthukumar M, Thalamadai Karuppiah M, Bhaskar Raju G (2007) Sep Purif Technol 55:198
3. Santos AB, Cervantes FJ, Lier JBV (2007) Bioresour Technol 98:2369
4. Oliveira DP, Carneiro PA, Sakagami MK et al (2007) Mutat Res Genet Toxicol Environ Mutagen 626:135
5. Hessel C, Allegre C, Maisseu M et al (2007) J Environ Manage 83:171
6. Forgacs E, Cserháti T, Oros G (2004) Environ Int 30:953
7. Mondal S (2008) Environ Eng Sci 25:383
8. Comninellis C, Chen G (2010) Electrochemistry for the environment, Springer, New York
9. Panizza M, Cerisola G (2009) Chem Rev 109:6541
10. Kapalka A, Fóti G, Comninellis C (2008) J Appl Electrochem 38:7
11. Cheng CY, Kelsall GH (2007) J Appl Electrochem 37:1203
12. Polcaro AM, Vacca A, Mascia M et al (2009) J Appl Electrochem 39:2083
13. Andrade LS, Ruotolo LAM, Rocha-Filho RC et al (2007) Chemosphere 66:2035
14. Andrade LS, Rocha-Filho RC, Bocchi N et al (2008) J Hazard Mater 153:252
15. Andrade LS, Tasso TT, Silva DL et al (2009) Electrochim Acta 54:2024
16. Mohd Y, Pletcher D (2006) Electrochim Acta 52:786
17. Panizza M, Cerisola G (2004) Environ Sci Technol 38:5470
18. Szpyrkowicz L, Kaul SN, Neti RN et al (2005) Water Res 39:1601
19. Montgomery DC (2009) Design and analysis of experiments, 7th edn. John Wiley & Sons, New York
20. Aquino JM, Rocha-Filho RC, Bocchi N et al (2010) J Braz Chem Soc 21:324
21. Alkan M, Celikcapa S, Demirbas O et al (2005) Dyes Pigm 65:251
22. Perkowski J, Kos L, Ledakowicz S et al (2003) Fibre Text East Eur 11:88
23. Vanhulle S, Enaud E, Trovaslet M et al (2008) Chemosphere 70:1097
24. Oliveira FH, Osugi ME, Paschoal FMM et al (2007) J Appl Electrochem 37:583
25. Alkan M, Oktay M, Kocakerim MM et al (2005) J Hazard Mater A119:13